Polymer Semiflexibility Induces Nonuniversal Phase Transitions in Diblock Copolymers

Shifan Mao,[1] Quinn MacPherson,[2] and Andrew J. Spakowitz[1,3,4]

[1]*Department of Chemical Engineering, Stanford University, Stanford, California 94305, USA*
[2]*Department of Physics, Stanford University, Stanford, California 94305, USA*
[3]*Department of Materials Science and Engineering, Stanford University, Stanford, California 94305, USA*
[4]*Department of Applied Physics, Stanford University, Stanford, California 94305, USA*

The order-disorder phase transition and the associated phase diagrams of semiflexible diblock copolymers are investigated using the wormlike chain model, incorporating concentration fluctuations. The free energy up to quartic order in concentration fluctuations is developed with chain-rigidity-dependent coefficients, evaluated using our exact results for the wormlike chain model, and a one-loop renormalization treatment is used to account for fluctuation effects. The chain length N and the monomer aspect ratio α directly control the strength of immiscibility (defined by the Flory-Huggins parameter χ) at the order-disorder transition and the resulting microstructures at different chemical compositions f_A. When monomers are infinitely thin (i.e., large aspect ratio α), the finite chain length N lowers the χN at the phase transition. However, fluctuation effects become important when chains have a finite radius, and a decrease in the chain length N elevates the χN at the phase transition. Phase diagrams of diblock copolymers over a wide range of N and α are calculated based on our fluctuation theory. We find that both finite N and α enhance the stability of the lamellar phase above the order-disorder transition. Our results demonstrate that polymer semiflexibility plays a dramatic role in the phase behavior, even for large chain lengths (e.g., $N \approx 100$).

Phenomenological theories for the thermodynamic behavior of molecular systems have had a profound influence on our understanding of phase transitions and critical phenomena. The dominant behavior in many systems is governed by large length-scale physical effects, leading to universal behaviors in macroscopically observable properties. However, the range of validity of phenomenological theories is not *a priori* known, and there exist few exact theoretical treatments that are capable of systematically introducing microscopic detail into the molecular model to probe the limits of a phenomenological treatment.

Block copolymer phase behavior, which has considerable fundamental and technological importance, represents a prototypical problem where much of our understanding hinges on coarse-grained, phenomenological models. Both experimental and theoretical studies have explored the phase diagram of diblock copolymers [1–3]. Random phase approximation (RPA) and self-consistent field theory (SCFT) are used to predict order-disorder transitions (ODTs) and melt microstructures above the phase transition [1,4,5], resulting in qualitative agreement of the phase diagram between experiments and mean-field theory. However, experimental phase transitions appear to be first order at all chemical compositions, and a mean-field treatment predicts a second-order phase transition for symmetric diblock copolymers. Mean-field theory also fails to predict the stable lamellar phase above the order-disorder transition for nearly symmetric chemical compositions. Furthermore, experiments observe that the ODT occurs at significantly lower temperature than predicted by mean-field theories [6].

To account for these discrepancies, theoretical studies turn to the effect of concentration fluctuations. The invariant degree of polymerization is defined as $\bar{N} = N\alpha^6$, where $\alpha = b/v^{1/3}$ is the ratio between the Kuhn statistical segment length b and the cube root of a monomer volume v, and $N = L/b$ is the number of Kuhn lengths for a polymer of length L. This quantity is used to characterize the effect of concentration fluctuations due to finite molecular weight [7–11]. Simulations based on bead-spring and on-lattice models show a universal ODT versus invariant degree of polymerization [12]. However, recently, Gillard *et al.* found nonuniversal features of phase transitions in polymers with low molecular weights [9]. Such observations are recently argued to be caused by chain polydispersity (i.e., a distribution of molecular weight) [13]. However, the dependence of the ODT on average molecular weight is not explored in that work, and the chain lengths that were simulated in Ref. [13] are as short as $N = 40$. In this work, we demonstrate that at such lengths polymer semiflexibility also plays a significant role in the behavior.

All theories mentioned above assume random-walk conformations of chains, which is only a valid assumption for sufficiently long diblock copolymers [14]. Ostensibly, the Kuhn length b identifies a length scale where the polymer transitions from a rigid chain to a flexible random

walk, but the range and impact of the crossover between these two limiting behaviors are not immediately clear. To find the effect of chain semiflexibility on the phase behavior of diblock copolymers, past studies used SCFT of wormlike chains [5,15–18], neglecting concentration fluctuations. Simulations of semiflexible copolymers [19–21] provide insight into the role of polymer rigidity in the morphology and the ODT. In this work, we aim to account for the finite molecular weight effects of diblock copolymers by considering the effects of chain semiflexibility and concentration fluctuations. We model the diblock copolymers as wormlike chains with finite bending rigidity. We use one-loop perturbation theory of the free energy with chain-rigidity-dependent coefficients to incorporate concentration fluctuation effects. We examine both the ODT and phase diagrams for microphase segregation, revealing nonuniversal phase behavior over a broad range of chain lengths N.

The wormlike chain model represents a polymer chain as a linear elastic thread subjected to thermal fluctuations [22,23]. However, an alternative view of the wormlike chain is that this model represents the lowest-order correction to the Gaussian chain model [23–25]. Generally, polymer chain behavior at intermediate length scales is captured by incorporating all quadratic-order deformation modes (bending, stretching, shearing, and bend-shear coupling) [24,25]. For simplicity, we assume the chains behave according to the inextensible wormlike chain model in this work [22,23].

Physical interactions between segments within flexible copolymers are frequently captured using a phenomenological isotropic interaction, formulated in terms of the segmental density or the local volume fractions of A-type and B-type segments. Since we consider the lowest-order correction to Gaussian-chain statistics, the treatment of interactions should also include a contribution from the local structural order arising from semiflexibility, which by symmetry is written as a local quadripole order parameter that characterizes the local alignment of the polymer chains [26]. Furthermore, polymer melts are frequently modeled as incompressible, which will break down at short length scales. In this work, we aim to capture the first correction to the thermodynamic behavior for non-Gaussian chains without resorting to detailed microscale interactions. Thus, we neglect the impact of the quadripole order parameter and melt compressibility in order to establish the dominant role of concentration fluctuations in copolymer phase behavior, and a future paper will focus on the influence of such effects.

We consider a diblock copolymer melt consisting of n_p semiflexible polymers. All polymers have identical chemical composition, with one A-type segment and one B-type segment. The fraction of the A-type polymer segment is denoted as f_A. The partition function of the polymer melt is written as

$$\mathcal{Z} = \int \prod_{j=1}^{n_p} \mathcal{D}\vec{u}_j(s) \exp\left[-\frac{l_p}{2}\sum_{j=1}^{n_p}\int_0^L ds\left(\frac{\partial \vec{u}_j(s)}{\partial s}\right)^2 - \frac{\chi}{2l_p A}\int d\vec{r}\hat{\phi}_A(\vec{r})\hat{\phi}_B(\vec{r})\right]\prod_{\vec{r}}\delta[\hat{\phi}_A(\vec{r}) + \hat{\phi}_B(\vec{r}) - 1].$$

(1)

The unit tangent vector $\vec{u}_j(s)$ at monomer position s (where $s \in [0, L]$) on the jth polymer defines the shape of the polymer chain. Each polymer is modeled as a wormlike chain with persistence length l_p (which scales with the chain rigidity and gives a Kuhn length $b = 2l_p$) and monomer cross-sectional area A. The δ-function constraint fixes $\hat{\phi}_A(\vec{r}) + \hat{\phi}_B(\vec{r}) = 1$ for all spatial positions $\vec{r}$, assuming incompressibility of the melt. The volume fraction of α-type monomers is given by

$$\hat{\phi}_\alpha(\vec{r}) = A\sum_{j=1}^{n_p}\int_0^L ds\sigma_\alpha(s)\delta[\vec{r} - \vec{r}_j(s)],$$

(2)

where $\sigma_\alpha(s)$ identifies whether the segment is α type at position s [i.e., $\sigma_A(s) = 1$ for $s < f_A L$ and $\sigma_A(s) = 0$ for $s \geq f_A L$].

Using RPA [3,4], the free-energy functional for the concentration order parameter $\psi(\vec{q})$ up to quartic order is written in Fourier space as [27]

$$\beta F[\tilde{\psi}] = \beta F_0 + \frac{1}{2}\int_{\vec{q}}\Gamma_2(\vec{q})\tilde{\psi}(\vec{q})\tilde{\psi}(-\vec{q})$$
$$+ \frac{1}{3!}\int_{\vec{q}_1,\vec{q}_2,\vec{q}_3}\Gamma_3(\vec{q}_1,\vec{q}_2,\vec{q}_3)\tilde{\psi}(\vec{q}_1)\tilde{\psi}(\vec{q}_2)\tilde{\psi}(\vec{q}_3)$$
$$+ \frac{1}{4!}\int_{\vec{q}_1,\vec{q}_2,\vec{q}_3,\vec{q}_4}\Gamma_4(\vec{q}_1,\vec{q}_2,\vec{q}_3,\vec{q}_4)\tilde{\psi}(\vec{q}_1)$$
$$\times \tilde{\psi}(\vec{q}_2)\tilde{\psi}(\vec{q}_3)\tilde{\psi}(\vec{q}_4),$$

(3)

where $\int_{\vec{q}}$ is shorthand for $\int (1/(2\pi)^3)d\vec{q}$, and the concentration order parameter $\tilde{\psi}(\vec{q})$ is the Fourier transform of deviation of local monomer concentration from its average value [i.e., $\psi(\vec{r}) = \phi_A(\vec{r}) - f_A = f_B - \phi_B(\vec{r})$].

The vertex functions [$\Gamma_n(\vec{q}_1, ..., \vec{q}_n)$ in Eq. (3)] are defined by Ohta and Kawasaki [27] and Leibler [4]. In evaluating the vertex functions, the 2-, 3-, and 4-point density correlation functions for a semiflexible chain are required. To achieve this, we extend our exact analytical solution of the single chain correlation functions from 2-points to 3- and 4-points on a single wormlike chain [28–31]. Detailed calculations of the multipoint correlation functions are shown in Supplemental Material [32], and our research group website [33] provides PYTHON scripts to evaluate the vertex functions.

We use the perturbative expansion of third- and fourth-order concentration fluctuations in Eq. (3) to find the

renormalized ODT and phase diagrams at different N and f_A at the one-loop approximation level. In our work, we employ the one-loop approximation employed by Fredrickson and Helfand [7], who used the Brazovskii approach [34] to account for concentration fluctuations of uniform and nonuniform phases.

The combined effects of molecular weight and monomer aspect ratio on the phase transition of symmetric diblock copolymers are shown in Fig. 1 based on one-loop predictions of $\chi_{\mathrm{ODT}}^{\mathrm{1L}}N$. Figure 1 provides $\chi_{\mathrm{ODT}}^{\mathrm{1L}}N$ versus molecular weight N in a range of monomer aspect ratios from $\alpha = 1, 2, 4, 8$, and 16 (red to blue). The mean-field result corresponding to the limit of the melt of infinitely thin polymers (i.e., $\alpha \to \infty$) is plotted in dashed black line.

The one-loop theory predicts that the phase transition to a lamellar phase occurs at $\chi_{\mathrm{ODT}}^{\mathrm{1L}}N = \chi_S^{\mathrm{MF}}(N)N + f(N, \alpha)$, where both terms on the right-hand side of the equation are dependent on finite molecular weight N. The mean-field spinodal $\chi_S^{\mathrm{MF}}(N)$ ranges from the rigid diblock copolymer limit ($\chi_S^{\mathrm{MF}}N \to 6.135$) for small N [5,15–17]) to the Gaussian chain limit ($\chi_S^{\mathrm{MF}}N \to 10.495$) for large N [3,4].

In the large-N limit, the solution by Brazovskii-Leibler-Fredrickson-Helfand (BLFH) theory using Gaussian chain conformation [7],

$$\chi_{\mathrm{ODT}}^{\mathrm{1L}}N = 10.495 + 41.0(N\alpha^6)^{-1/3}, \qquad (4)$$

is recovered. Considering chain semiflexibility, we find more pronounced elevation of $\chi_{\mathrm{ODT}}^{\mathrm{1L}}N - \chi_S^{\mathrm{MF}}N$. Particularly in the rigid rod limit, we find

$$\chi_{\mathrm{ODT}}^{\mathrm{1L}}N = 6.135 + 76.9(N\alpha^{3/2})^{-4/3}. \qquad (5)$$

Determination of the scaling laws for $\chi_{\mathrm{ODT}}^{\mathrm{1L}}N - \chi_S^{\mathrm{MF}}N$ is detailed in Supplemental Material [32]. Physically, large α
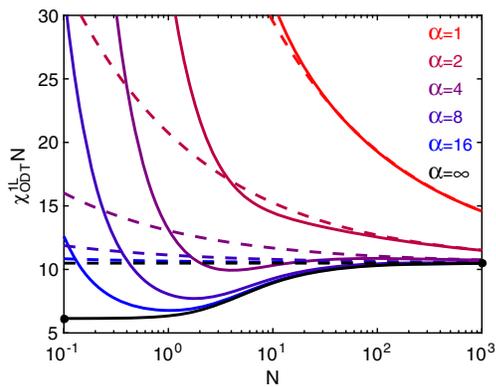

FIG. 1. Phase transition $\chi_{\mathrm{ODT}}^{\mathrm{1L}}N$ (predicted using one-loop renormalization theory) of a symmetric semiflexible diblock copolymer at different monomer aspect ratio α (in colors). Solid curves correspond to our theory of semiflexible polymers, and the dashed curves are predictions from a flexible polymer treatment [Eq. (4)] [7].

coincides with a larger number of interactions between neighboring chains at local length scales (i.e., comparable to $b = 2l_p$), suppressing the role of concentration fluctuations (i.e., more mean-field-like). Thus, the local chain configuration dictated by semiflexibility dominates the behavior for small N. Conversely, small α has fewer neighboring-chain interactions, and fluctuation effects dominate the thermodynamic behavior before chain rigidity influences the microstructure at small N.

This significant renormalization of the ODT for semiflexible diblock copolymers stresses the importance of concentration fluctuation effects when chain molecular weights become small. However, these predictions exhibit a notable influence of semiflexibility for relatively large N, with a reduction in $\chi_{\mathrm{ODT}}^{\mathrm{1L}}N$ beginning at $N \approx 100$ for large α.

We examine the phase diagrams of diblock copolymers of different molecular weights and monomer aspect ratios. Figure 2 shows the phase diagrams of diblock copolymers with molecular weights $N = 10, 50$, and 100, and monomer aspect ratios $\alpha \to \infty$ (mean-field solutions), $\alpha = 4$, and $\alpha = 2$. These N values are chosen to be significantly larger than $N = 1$ in order to emphasize the impact of semiflexibility even for large chain lengths. The mean-field phase diagrams are constructed based on wave mode analysis based on free energy with full angular dependences of Γ_3 and Γ_4. The phase diagrams with finite α are made according to a Hartree approximation [7,34].

When $N = 100$, the mean-field phase diagram is quantitatively the same as the phase diagram in Fig. 8 in Ref. [4]. The body-centered-cubic phase (labeled B in Fig. 2) is the first stable phase above the mean-field spinodal at $f_A \neq 0.5$, and the cylindrical phase (labeled C) and lamellar phase (labeled L) become more stable at higher χ, depending on chemical composition f_A. With decreasing molecular weight, the mean-field χN at the spinodal decreases at all chemical composition f_A. However, the relative width of the lamellar phase is qualitatively the same as that of long polymers. The phase diagram of diblock copolymers with $N = 10$ qualitatively agrees with that from Refs. [16,17].

For polymers with 100 Kuhn steps and monomer aspect ratio $\alpha = 4$, fluctuation effects destroy the critical point, and the χN at the phase transition is elevated most noticeably near $f_A = 0.5$. The lamellar phase becomes the first stable phase above the ODT for nearly symmetric diblock copolymers. At smaller monomer aspect ratio ($\alpha = 2$), the body-centered-cubic phase is eliminated from the phase diagram, which predicts a qualitatively different phase behavior than the mean-field prediction. These trends for sufficiently long polymers is consistent with the BLFH theory based on Gaussian chains [7].

Similar to long polymers (i.e., $N = 100$), fluctuations destroy the critical points for polymers of length $N = 50$ and 10. The elevation of the phase transition near a
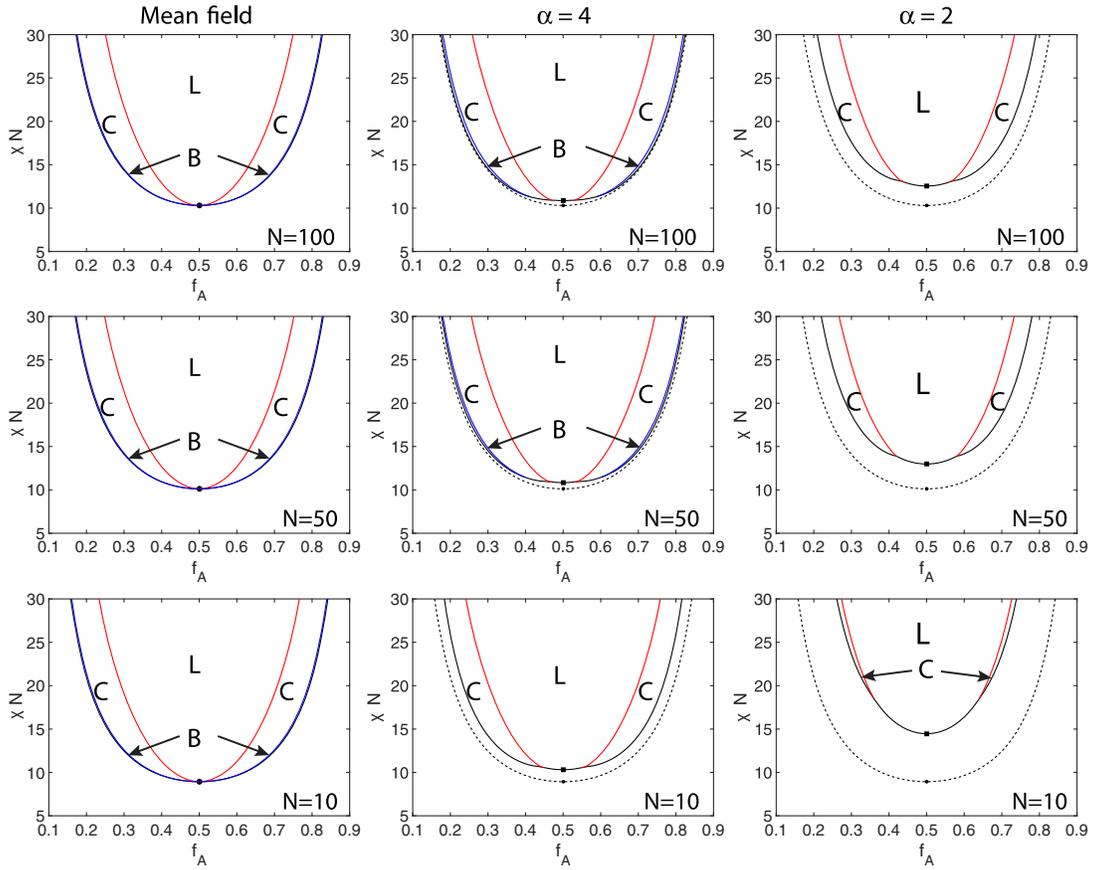
FIG. 2. Phase diagrams of diblock copolymers with varying molecular weights N and monomer aspect ratio α. Letters (with arrows) indicate lamellar (L), body-centered-cubic (B), and hexagonally packed cylinder (C) phases. The dashed lines at $\alpha = 2, 4$ are mean-field spinodals. The circles indicate mean-field critical points χ_S^{MF} ($f_A = 0.5$), and the squares are one-loop ODTs at symmetric composition χ_{ODT}^{1L} ($f_A = 0.5$).

symmetric composition is more pronounced for short polymers than that of long polymers, since fluctuations are more significant for short polymers. The lamellar phase domain is enlarged by smaller molecular weight when fluctuations are captured (i.e., finite α), resulting in a smaller region of the phase diagram for the cylindrical phase and the absence of the body-centered-cubic phase. This is because cylindrical and body-centered-cubic phases have smaller surface free energy per chain than the lamellar phase [14]. Thus, upon introduction of concentration fluctuations, cylindrical and body-centered-cubic phases are less stable than lamellar phases.

The Gaussian chain model does not capture all the microscropic details of the polymers due to chain semi-flexibility at sufficiently short length scales. When considering the concentration fluctuation effects, the small length-scale contributions introduce a UV divergence [35], requiring regularization techniques to account for the divergence systematically. Similar to Gaussian chains, the wormlike chain model is not free from this UV divergence. In fact, UV divergence becomes more significant as the wavelength (i.e., $2\pi/q$) approaches the

persistence length, since the wormlike chain model predicts a scaling of $\langle \tilde{\psi}^2(q) \rangle \sim q^{-1}$ in the limit $q \gg 1/l_p$. Future work will focus on the UV divergence of semiflexible polymers with the goal of developing a cutoff independent theory for phase behavior of copolymers.

In this Letter, we address the phase behavior of semiflexible diblock copolymers using our exact results for the wormlike chain within a field-theoretic treatment. Our theory accounts for polymer semiflexibility and fluctuation effects at short length scales, or equivalently for short polymers. The result of this theory shows the breakdown of the universal phase behavior of diblock copolymers proposed by earlier works. With the technological trend of engineering materials and devices with smaller length-scale features, our work provides evidence of the necessity of incorporating microscopic details in studying the thermodynamics of copolymers and soft materials, even when the feature size is significantly larger than the microscopic correlation length (e.g., the Kuhn length). Furthermore, this work provides a prototypical example for addressing where microscopic detail begins to influence macroscopic thermodynamic behavior.

[1] F. S. Bates and G. H. Fredrickson, Annu. Rev. Phys. Chem. **41,** 525 (1990).

[2] Y. Mai and A. Eisenberg, Chem. Soc. Rev. **41,** 5969 (2012).

[3] G. Fredrickson, in *The Equilibrium Theory of Inhomogeneous Polymers*, International Series of Monographs on Physics (Oxford University Press, New York, 2013).

[4] L. Leibler, Macromolecules **13,** 1602 (1980).

[5] M. Matsen, J. Chem. Phys. **104,** 7758 (1996).

[6] F. S. Bates, M. F. Schulz, A. K. Khandpur, S. Förster, J. H. Rosedale, K. Almdal, and K. Mortensen, Faraday Discuss. **98,** 7 (1994).

[7] G. H. Fredrickson and E. Helfand, J. Chem. Phys. **87,** 697 (1987).

[8] J. Qin and D. C. Morse, Phys. Rev. Lett. **108,** 238301 (2012).

[9] T. M. Gillard, P. Medapuram, D. C. Morse, and F. S. Bates, Macromolecules **48,** 2801 (2015).

[10] B. Vorselaars, P. Stasiak, and M. W. Matsen, Macromolecules **48,** 9071 (2015).

[11] J. Glaser, J. Qin, P. Medapuram, M. Müller, and D. C. Morse, Soft Matter **8,** 11310 (2012).

[12] J. Glaser, P. Medapuram, T. M. Beardsley, M. W. Matsen, and D. C. Morse, Phys. Rev. Lett. **113,** 068302 (2014).

[13] T. M. Beardsley and M. W. Matsen, Phys. Rev. Lett. **117,** 217801 (2016).

[14] M. W. Matsen, J. Phys. Condens. Matter **14,** R21 (2002).

[15] S. Li, Y. Jiang, and J. Z. Chen, Soft Matter **10,** 8932 (2014).

[16] Y. Jiang and J. Z. Y. Chen, Phys. Rev. E **88,** 042603 (2013).

[17] Y. Jiang and J. Z. Y. Chen, Phys. Rev. Lett. **110,** 138305 (2013).

[18] N. A. Kumar and V. Ganesan, J. Chem. Phys. **136,** 101101 (2012).

[19] J. Song, T. Shi, Y. Li, J. Chen, and L. An, J. Chem. Phys. **129,** 054906 (2008).

[20] R. A. Lawson, A. J. Peters, B. Nation, P. J. Ludovice, and C. L. Henderson, J. Micro/Nanolithogr. MEMS MOEMS **13,** 031308 (2014).

[21] S. Mao, Q. MacPherson, and A. Spakowitz, Macro Lett. **7,** 59 (2018).

[22] O. Kratky and G. Porod, Recl. Trav. Chim. **68,** 1106 (1949).

[23] N. Saito, K. Takahashi, and Y. Yunoki, J. Phys. Soc. Jpn. **22,** 219 (1967).

[24] E. F. Koslover and A. J. Spakowitz, Macromolecules **46,** 2003 (2013).

[25] E. F. Koslover and A. J. Spakowitz, Soft Matter **9,** 7016 (2013).

[26] A. J. Spakowitz and Z.-G. Wang, J. Chem. Phys. **119,** 13113 (2003).

[27] T. Ohta and K. Kawasaki, Macromolecules **19,** 2621 (1986).

[28] A. J. Spakowitz and Z.-G. Wang, Macromolecules **37,** 5814 (2004).

[29] A. J. Spakowitz and Z.-G. Wang, Phys. Rev. E **72,** 041802 (2005).

[30] A. J. Spakowitz, Europhys. Lett. **73,** 684 (2006).

[31] S. Mehraeen, B. Sudhanshu, E. F. Koslover, and A. J. Spakowitz, Phys. Rev. E **77,** 061803 (2008).

[32] See Supplemental Material at http://link.aps.org/supplemental/10.1103/PhysRevLett.120.067802 for detailed analytical calculations of multipoint correlation functions of wormlike chains, and vertex functions of semiflexible diblock copolymers. It also shows examples of structure factors, scaling of phase transition χN in N, and demonstrates UV divergence of semiflexible diblock copolymers.

[33] A. J. Spakowitz, http://www.stanford.edu/~ajspakow/.

[34] S. Brazovskii, Sov. J. Exp. Theor. Phys. **41,** 85 (1975).

[35] A. Kudlay and S. Stepanow, J. Chem. Phys. **118,** 4272 (2003).